Characterizing Interactions between Suwannee River Dissolved Organic Matter and Cu(II) Using Fluorescence Excitation–Emission Matrices and Parallel Factor Analysis

Mingquan Yan[1*], Xiaona Ma[2], Jixia Cheng[3]

[1]Department of Environmental Engineering, Peking University, The Key Laboratory of Water and Sediment Sciences, Ministry of Education, Beijing 100871, China

[2]Sinosteel Engineering Design and Research Institute Co., Ltd, Beijing 100080, China

[3] College of Environmental Sciences and Engineering, Chang'an University, Xi'an, Shaanxi, 710064, China

ABSTRACT

This study investigated the binding of Cu(II) to dissolved organic matter (DOM) using the method of fluorescence excitation–emission matrix (EEM) combined with parallel factor analysis (PARAFAC). The examined DOM samples included Suwannee River natural organic matter (SRNOM), humic acid (SRHA), fulvic acid (SRFA) and hydrophilic acid (SRHPiA). The differences in metal binding properties were discerned via the behavior of individual groups of DOM fluorophores. PARAFAC examination showed that there were up to seven independent EEM components that behave differently in terms of the effects of Cu(II) on their fluorescence intensity. Component 1 ($\lambda_{ex}/\lambda_{em}$ = (270, 340, 395) nm /~500 nm) and Component 2 ($\lambda_{ex}/\lambda_{em}$ = (~240, 330) nm /~450 nm) were found to be responsive to Cu(II) binding in all four DOM samples. Component 3 ($\lambda_{ex}/\lambda_{em}$ = (220, 270-310) nm/400 nm) was present in the case of Cu(II) binding to SRNOM, SRFA, and SRHPiA. Component 4 ($\lambda_{ex}/\lambda_{em}$ = (260, 340) nm /470 nm), Component 5 ($\lambda_{ex}/\lambda_{em}$ = (220, 245, 280) nm /420 nm), and Component 6 ($\lambda_{ex}/\lambda_{em}$ = (220, 260, 340) nm /420 nm) were found in Cu(II) binding to SRNOM and SRHA, while Component 7 ($\lambda_{ex}/\lambda_{em}$ = (220, 260-340) nm/430 nm) emerged as a result of in Cu(II) binding to SRFA and SRHPiA. The apparent equilibrium constants of Cu(II) binding to each PARAFAC-discerned component were determined using the Ryan and Weber equation, and the corresponding log K values were in the range of 4.9-6.1 while the percentage of fluorescence intensity (f)that was quenched by Cu(II) was in the range of 0.45-0.99 for different DOM components discerned by PARAFAC. The results demonstrate that PARAFAC analysis of metals affecting on DOM EEM is a promising approach to gain better insight into the interactions between trace metals and specific groups of DOM fluorophores.

Keywords: EEM; PARAFAC; copper; complexation; dissolved organic matter

1. INTRODUCTION

Dissolved organic matter (DOM) found in all natural waters is a complex entity comprised by compounds with varying molecular weights and diverse functionalities (e.g., carboxyl, phenol, enol, alcohol, carbonyl, amine, and thiol) (Chen et al., 2003; Leenheer and Croue, 2003). Chemical and physical characteristics of DOM play an important role in its interactions with metals affecting their environmental fate, bioavailability and toxicity (Bai et al., 2008; Baken et al., 2011; Leenheer and Croue, 2003; Wu et al., 2004). The binding of metals to unfractionated DOM and its representative

fractions has been extensively studied using a wide range of techniques, for instance potentiometric titration, voltammetry, fluorescence spectroscopy, ion exchange, gel filtration, dialysis, ultrafiltration, electron spin resonance spectroscopy, extended X-ray absorption fine structure, etc. A large variety of thermodynamic equilibrium constants obtained using these approaches and their sometime divergent interpretations have been reported (Browne and Driscoll, 1993; Cabaniss, 1992; Chen et al., 2003; Gamble et al., 1980; Gustafsson and Kleja, 2005; Korshin et al., 2009; Pullin and Cabaniss, 1995; van Schaik et al., 2008; Wu et al., 2004).

Examination of the effects of metals on the fluorescence of DOM is one of the most extensively utilized methods to probe DOM-metal interactions and estimate the corresponding equilibrium constants (Esteves da Silva et al., 1998; Seredyńska-Sobecka et al., 2011; Wu et al., 2011). This technique quantifies the quenching or enhancement of DOM fluorescence caused by DOM-metal complexation. The parameters describing these equilibria, typically a single discrete complexation constant log K and DOM complexation capacity (CC), are frequently determined using an equation that relates changes of DOM fluorescence at its maximum and log K and CC values (Cabaniss, 1992; Leenheer and Croue, 2003; Ryan and Weber, 1982). Measurements of synchronous fluorescence spectra and excitation-emission matrix (EEM) (Cabaniss, 1992; Cook and Langford, 1995; Chen et al., 2003; Esteves da Silva et al., 1998; Kumke et al., 1998; Luster et al., 1996; Mobed et al., 1996; Pullin and Cabaniss, 1995; Plaza et al., 2006; Reynolds, 2003) have demonstrated that different peaks in synchronous fluorescence spectra of DOM or different regions of EEM were quenched to different degree, clearly indicating different types of interactions between the metals and DOM fluorophores associated with these features.

EEM "landscapes" have been typically characterized by the coordinates and intensities of one or more peaks that are universally present in EEM of DOM (Coble, 1996; Luster et al., 1996; Patel-Sorrentino et al., 2002; Plaza et al., 2006). Because these peaks tend to be relatively broad and overlapping, and their intensities exhibit varying sensitivities to interactions with metal ions, the selection of the excitation/emission pairs at which the metal binding by DOM is quantified may be subjective and result in incomplete evaluation of the relevant metal-DOM interactions. However, since the synchronous fluorescence spectra and EEMs comprise overlapping features corresponding to contributions of various fluorophores, better resolution is required to obtain accurate binding parameters.

These limitations can be addressed via the analysis of entire EEM datasets, as opposed to that of the fluorescence intensity at one or more discrete $\lambda_{ex}/\lambda_{em}$ pairs. This was demonstrated in the studies by Ohno et al. (2008), Yamashita and Jaffe (2008) and Wu et al. (2011), who used parallel factor analysis (PARAFAC) to deconvolute EEMs generated for DOM samples originating from a certain natural environment into contributions of independent groups of DOM fluorophores. This approach was combined with measurements of fluorescence quenching at $\lambda_{ex}/\lambda_{em}$ combinations corresponding to each DOM fluorophore group to assess the interaction of these fluorophore groups with metals. However, the precision of this approach may be still affected by the overlap of dissimilar DOM fluorophores that can take place at any $\lambda_{ex}/\lambda_{em}$ combination (Ohno et al., 2008; Wu et al., 2011; Yamashita and Jaffe, 2008). This limitation can be addressed via rigorous analysis of the behavior of the responses of entire groups of DOM fluorophores whose engagement contributions can be probed at varying metal loads, but this approach has not been utilized with adequate consistency in relevant research.

In this paper, we investigated the binding of Cu(II) by DOM using EEM and PARAFAC analysis of absolute and relative changes of EEM intensities caused by metal ions' interactions with different DOM fluorophores. EEMs for representative DOM samples, including IHSS standards (Suwannee River natural organic matter (SRNOM), humic acid (SRHA), fulvic acid (SRFA) and hydrophilic acid (SRHPiA)) were generated and used to compare the contributions of their constituents and apparent complexation constants associated Cu(II) binding by them. The intent of this study is to provide additional EEM data and their analysis to better understand interactions between metal and individual fluorescent components of DOM in aquatic environments.

2. METHODS AND MATERIALS

2.1 Reagents and chemicals

All chemicals were AR grade unless mentioned otherwise. All solutions were prepared using Milli-Q water (18.2 MΩ cm^{-1}, MilliporeCorp., MA, USA), including 0.0001, 0.001 and 0.005 L^{-1} Cu(ClO$_4$)$_2$; 0.01 and 0.1 mol L^{-1} of NaOH; and 0.01, 0.1 and 1.0 mol L^{-1} of HClO$_4$.

2.2 Samples

Suwannee River natural organic matter (SRNOM) (1R101N), Suwannee River humic acid (SRHA) (1R101H) and Suwannee River fulvic acid (SRFA) (1S101F) were obtained from the International Humic Substances Society (IHSS). Suwannee River hydrophilic acid (SRHPiA) was obtained by passing an acidified (pH 2) sample of Suwannee River organic matter eluted from column containing Amberlite XAD-8 resin through a column containing Amberlite XAD-4 resin and then eluting the fraction absorbed on XAD-4 resin with sodium hydroxide. SRNOM, SRHA, SRFA and

SRHPiA solutions were prepared at a 5 mg L^{-1} DOC concentrations with Millipore Milli-Q (MQ) water. To minimize hysteresis effects (Dryer et al., 2008), the solution pH was cycled between 2 and 11 four times prior to the titration analysis. During this cycling, the solution pH was held at each end point for 30 min to allow for potentially slow equilibration of the molecules of humic acids. Background ionic strengths were established by inclusion of 0.04 M NaClO$_4$ as background electrolyte (AR grade). Concentrations of dissolved organic carbon (DOC) were analyzed using a Shimadzu TOC-Vcsh carbon analyzer.

2.3 Titration

Cu(II) titrations were processed by adding appropriate volumes of prepared Cu(II) stock solution into 100 ml DOM solutions to obtain sequentially increasing Cu(II) concentration from 0 to about 25.6 µM at temperature 25 °C. The pH of the solutions was kept at pH 5.0 during Cu(II) additions, and it was controlled through addition of small amounts of dilute HClO$_4$ or NaOH if necessary. The containers were continuously stirred during experiments and were open to the atmosphere. After each addition of Cu(II), the solution was allowed equilibrating for 30 min prior to the removal of 1 mL aliquots for fluorescence EEM analysis, the aliquots were added back to the solution prior to the next addition of Cu(II) titration.

2.4 Fluorescence scans

Fluorescence EEM data were obtained using a Perkin-Elmer LS 50B Luminescence spectrometer (with a 1 cm cell). EEM acquisition involved scanning and recording of 40 individual emission spectra at sequential 5 nm increments of excitation wavelength (λ_{ex}) between 220 and 415 nm. The emission wavelength (λ_{em}) range set from 350 to 580 nm in 0.5 nm increments. Instrumental parameters were excitation and emission slits, 5 nm; and

scan speed, 1200 nm min^{-1}.

2.5 PARAFAC modeling

The approach of PARAFAC modeling of EEMs followed the procedure described in detail by Stedmon and Bro (2008) and Ohno et al. (2008), and only a brief description was given here. Essentially, PARAFAC examines a consistent series of EEM landscapes formed a so-called three-way array of size $I \times J \times K$, where J is the number of emission wavelengths, K is the number of excitation wavelengths, and I is the number of samples, which is corresponding to the fluorescence EEM landscape measured of DOM samples in the absence and with addition of various concentrations of Cu(II) in this study. It provides an estimate of the number of independent fluorophores as well as their excitation and emission spectra, and also provides relative contributions (or concentrations) of each fluorophore in the samples.

Corrections for Raman scattering were obtained by subtracting water blanks. The higher intensity Rayleigh scatter lines were removed by replacing the fluorescence intensity values with missing values in the region immediately adjacent to where emission wavelength was equal to 1 and 2 times the excitation wavelength. The EEM spectra had a triangularly shaped region where the emission wavelength was less than that of the excitation wavelength. Because such a characteristic is not expected for DOM solutions, thus these data pairs were set to zero.

PARAFAC modeling was carried out in MATLAB 2010a (Mathworks, Natick, MA) with N-way toolbox and DOM Fluor toolbox (Stedmon and Bro, 2008). A non-negativity constraint was applied to the parameters to allow only chemically and spectroscopically relevant results (Stedmon and Bro, 2008).

2.6 Complexation modeling

The complexation model reported by Ryan and Weber (1982) was used to determine the binding parameters between fluorescent components derived from PARAFAC and metals. This simple but widely used model is based on the assumption of the formation of 1:1 complexes between ligands and trace metals. According to Ryan and Weber hypothesis (Esteves da Silva et al., 1998; Ryan and Weber, 1982; Yamashita and Jaffe, 2008), the following relationship between the fluorescence intensity (I) and the total metal ion concentration (C_M) is obtained.

$$I = I_0 + \frac{(I_{ML} - I_0)1}{2KC_L}(1 + KC_L + KC_M - \sqrt{(KC_L + KC_M + 1)^2 - 4K^2 C_L C_M})$$

(1)

where I and I_0 are the fluorescence intensity at the metal concentration C_M and at the beginning of titration (in the absence of added metals), respectively. I_{ML} is the limiting value below which the fluorescence intensity does not change due to the addition of metal. K and C_L are the conditional stability constant and total ligand concentration, respectively. K, C_L and I_{ML} were obtained via nonlinear regression analysis of the equation using MATLAB 2010a. In addition, the fraction of the initial fluorescence that corresponds to the binding fluorophores (f) was determined using equation 2.

$$f = \frac{(I_0 - I_{ML})}{I_0} \times 100$$

(2)

3. RESULTS AND DISCUSSION

3.1 EEM landscape of DOMs

EEM landscapes of SRNOM, SRHA, SRFA and SRHPiA at pH 5.0 in the absence of Cu(II) are shown in Figure 1 (a), (b), (c), and (d). The EEM data for the four Suwannee River DOM

samples had substantial similarities such as the presence of two prominent peaks (referred to as Peak A, $\lambda_{ex}/\lambda_{em}$ = 245-260 nm/420-460 nm, Peak B, $\lambda_{ex}/\lambda_{em}$ = 325-340 nm/420-460 nm) and a shoulder at $\lambda_{ex}/\lambda_{em}$ = 325-340 nm/450-490 nm (Peak C). Peaks A and B observed in these experiments were similar to those described in the previous studies that utilized samples of highly variable origins (commercial humic substances, fresh water, seawater or coastal organic matter) (Coble, 1996; Christensen et al., 2005; Cory and McKnight, 2005; Hall et al., 2005; Ohno and Bro, 2006). Although the DOC concentrations were the same in all cases (5.0 mg L^{-1}), the intensities of fluorescence of SRFA and

SRHPiA were considerably higher than those of SRNOM and SRHA.

The addition of Cu(II) led to the appearance of two new local maxima in the EEM of SRNOM and SRHA located at $\lambda_{ex}/\lambda_{em}$ = 280 nm/420 nm, and $\lambda_{ex}/\lambda_{em}$ = 250 nm/420 nm, while the intensity of the rest of the EEM of SRNOM and SRHA decreased with the addition of Cu(II). In contrast with the behavior of SRNOM and SRHA, the addition of Cu(II) to the SRFA and SRHPiA solutions caused a significant reduction of the intensities of Peaks A and B, but no additional features appeared (Shown in Figure 1 (e), (f), (g), and (h) for SRNOM, SRHA, SRFA and SRHPiA, respectively).
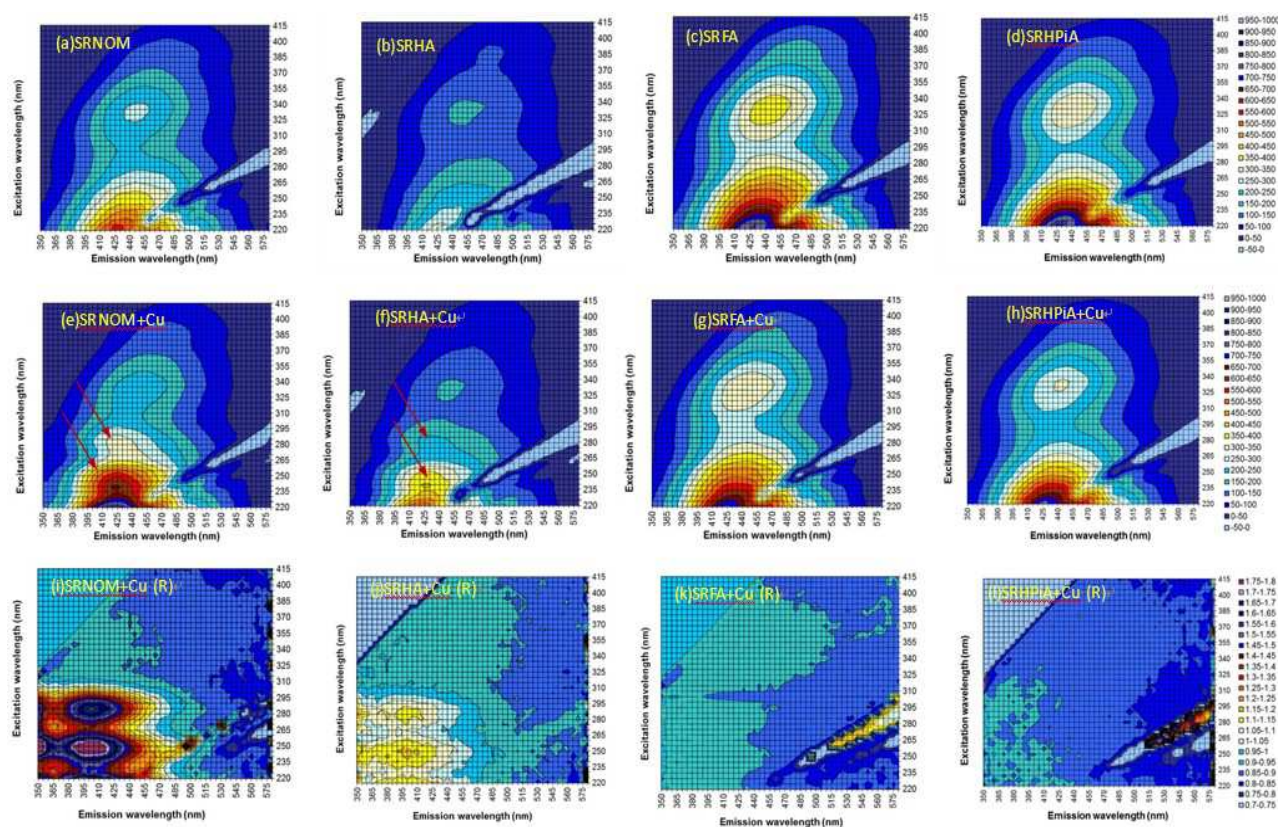

Figure 1   EEM data in the absence of Cu(II) for SRNOM (a), SRHA (b), SRFA (c), and SRHPiA (d); EEM data in the presence of 1.6 µM Cu(II) for SRNOM (e), SRHA (f), SRFA (g), and SRHPiA (h); relative changes of the EEM in the presence of 1.6 µM Cu(II) of SRNOM (i), SRHA (j), SRFA (k), and SRHPiA (l), calculated using the reference EEM corresponding to in the absence of Cu(II)

The changes of EEM spectra after the addition of Cu(II) were affected by DOM properties. In order to examine in more detail the nature of the changes of fluorescence intensity caused by the presence of Cu(II), the EEM data set generated in the presence of 1.6 µM Cu(II) was normalized by the EEM data in the absence of Cu(II). This procedure allowed generating 3D matrixes of relative changes of DOM fluorescence after the addition of Cu(II). Examination of these matrixes of relative EEM sensitivities allowed establishing important features in the relevant EEM regions.

The 3D maps relative changes of DOM fluorescence quenching or enhancement in the presence of 1.6 µM Cu(II) are shown in Figure 1 (i), (j), (k), and (l) for SRNOM, SRHA, SRFA, and SRHPiA, respectively. It shows that the addition of small amounts of Cu(II) to SRNOM and SRHA led to the appearance of four peaks of relatively increased intensity (Figure 1 (i) and (j)). These peaks had coordinates of $\lambda_{ex}/\lambda_{em}$ = 280 nm/350 nm, $\lambda_{ex}/\lambda_{em}$ = 250 nm/350 nm and $\lambda_{ex}/\lambda_{em}$ = 280 nm/400 nm, $\lambda_{ex}/\lambda_{em}$ = 240 nm/400 nm. The location of these local maxima of relative fluorescence increases was different from that of the maxima of absolute EEM intensity shown in Figure 1 (e) and (f). In the other EEM regions of SRNOM and SRHA, the intensity of fluorescence decreased with the addition of Cu(II), however, the relative sensitivity of EEM intensity to the presence of Cu(II) was not uniform, and the quenching by Cu(II) was more prominent at higher emission wavelength (Balistrieri and Blank, 2008; Cabaniss, 2011; Di Toro et al., 2001; Meylan et al., 2004).

In contrast with the data for SRNOM and SRHA, the fluorescence intensity of SRFA and SRHPiA decreased in the entire range of excitation and emission wavelengths with the addition of Cu(II) (Figure 1 (k) and (l)). Similarly to the observation for SRNOM and SRHA, the quenching of SRFA and SRHPiA

emission was more pronounced at higher emission wavelength.

3.2 Quantitation of interactions of Cu(II) with DOM

To ascertain the behavior of the fluorophores contributing to the EEM of the each studied DOM sample, the entire set of the EEM data generated using varying concentrations of Cu(II) was examined by PARAFAC. The PARAFAC models with 2-6 components were computed for the SRNOM, SRHA, SRFA, and SRHPiA data sets separately. In the case of Cu(II) binding, seven PARAFAC components were determined to be present in the examined samples, with varying prominence and numbers in different samples. These components are shown in Figure 2.

Six components were present in the EEM of SRNOM, including five components for SRHA and four components for SRFA and SRHPiA, respectively. The appropriate number of components was chosen sufficiently high to fully describe the systematic variation in the data to the point where the assumptions of trilinearity became invalid, i.e. core consistency diagnostic score became low and residual analysis reached minimum. The core consistency diagnostic score was > 90%, and the sum of squared error was < 105 for each data set, thus the error was acceptable (Wu et al., 2011). The sum of squared error is shown in Figure 3. Component 1 ($\lambda_{ex}/\lambda_{em}$ = (270, 340, 395) nm/~500 nm) and Component 2 ($\lambda_{ex}/\lambda_{em}$ = (~240, 330) nm/~450 nm) were present in the responses of all four DOM samples to Cu(II) binding. Component 3 ($\lambda_{ex}/\lambda_{em}$ = (220, 270-310) nm/400 nm) was found for SRNOM, SRFA, and SRHPiA. Component 4 ($\lambda_{ex}/\lambda_{em}$ = (260, 340) nm/470 nm), Component 5 ($\lambda_{ex}/\lambda_{em}$ = (220, 245, 280) nm/420 nm), and Component 6 ($\lambda_{ex}/\lambda_{em}$ = (220, 260, 340) nm/420 nm) were found in Cu(II) binding to SRNOM and

SRHA, while Component 7 ($\lambda_{ex}/\lambda_{em}$ = (220, 260-340) nm/430 nm) was only found in Cu(II) binding to SRFA and SRHPiA.

The maximum fluorescence intensities of each PARAFAC component associated with changes of EEM caused by the addition of Cu(II) are shown in Figure 4 (a), (d), (g), and (j) for SRNOM, SRHA, SRFA, and SRHPiA, respectively. The model predictions generated based on the Ryan-Weber equation (eq.1) are shown as well.

The fluorescence intensity of the PARA-FAC-discerned components decreased gradually with the addition of Cu(II), except for Component 4 and Component 5 in SRNOM and SRHA. Conditional stability constants (log K) and the fraction of the fluorescence intensity (f) of each EEM component that was affected by Cu(II) complexation were determined using eq. 1 and eq. 2 and are shown in Table 1.
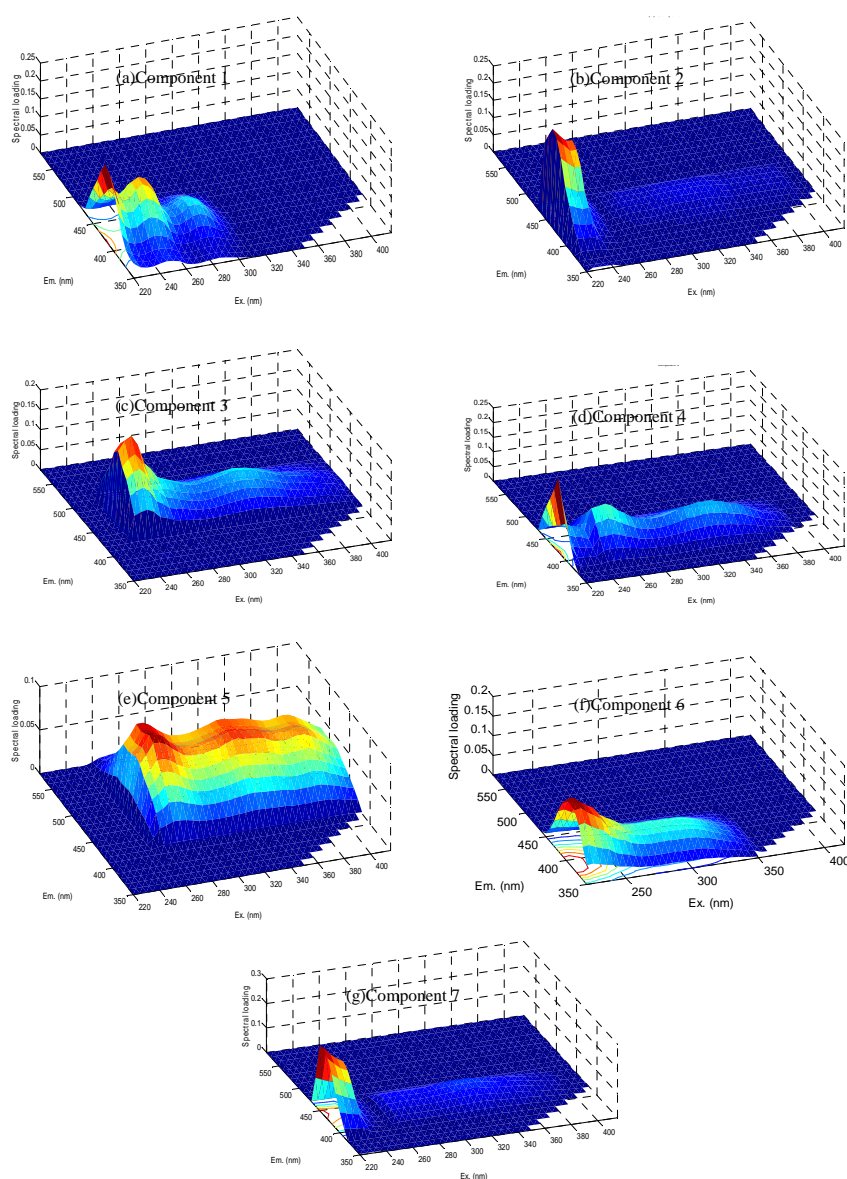

Figure 2   Excitation and emission spectral loadings of the non-negatively on strained PARA-FAC model components of Cu(II) complex to DOMs
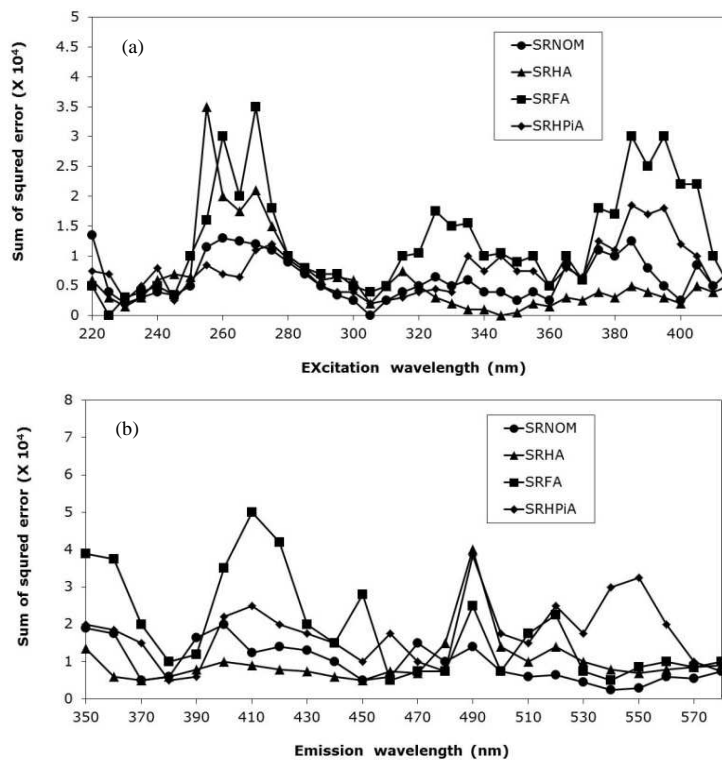
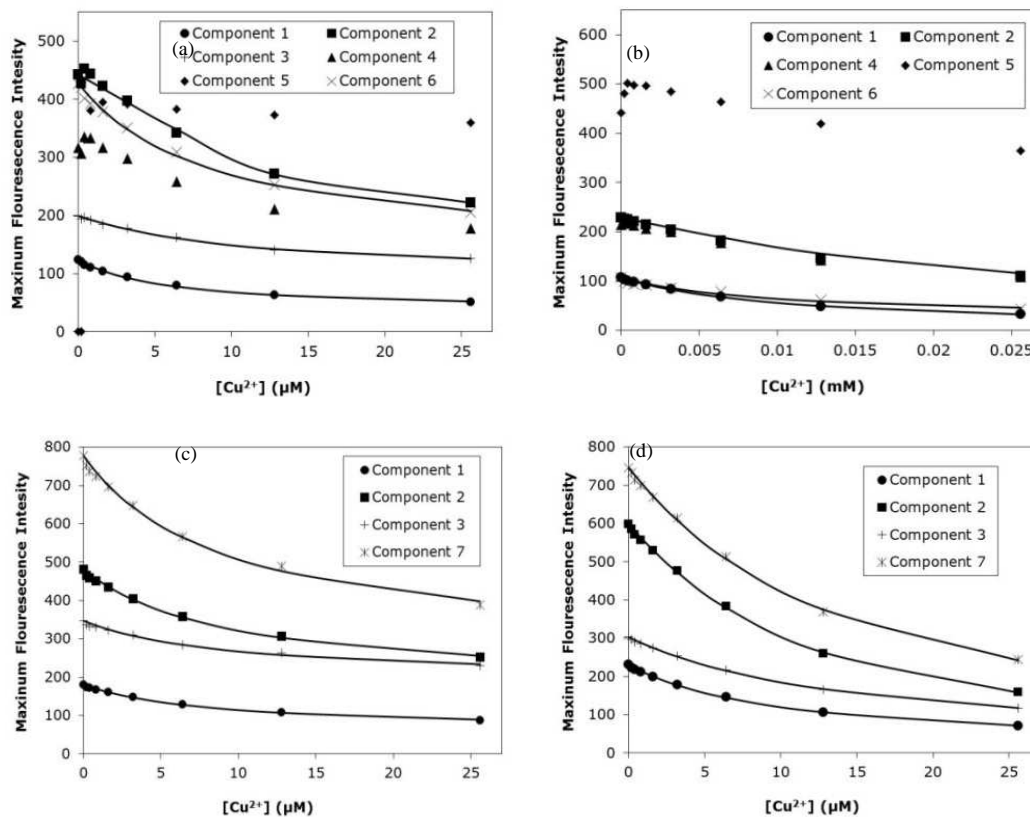**Figure 3**　Residual analysis of model components by EEM-PARAFAC for SROMs

Figure 4　Maximum fluorescence intensity of PARAFAC model components complex to SRNOM (a), SRHA (b), SRFA (c), and SRHPiA (d), respectively, values calculated by PARA-FAC (dots) and predicted by Ryan and Weber model (solid line)

Table 1 Fitting parameters of the Ryan-Weber model, i.e., percentage of fluorescence intensity participating in the binding (f), stability constant (log K), and correlation coefficient of predicted vs. measured fluorescence intensity (R^2)

DOM sample	SRNOM			SRHA			SRFA			SRHPiA		
parameter	Log K	f	R^2	Log K	f	R^2	Log K	f	R^2	Log K	f	R^2
Component 1	5.24	0.71	0.99	4.96	0.99	1.00	5.08	0.67	1.00	5.00	0.96	1.00
Component 2	6.14	0.53	0.99	5.36	0.68	1.00	5.03	0.64	0.99	5.15	0.98	1.00
Component 3	5.12	0.49	1.00	Not found			5.02	0.45	0.99	4.89	0.94	1.00
Component 4	No model			No model			Not found			Not found		
Component 5	No model			No model			Not found			Not found		
Component 6	5.06	0.69	0.99	5.02	0.78	0.94	Not found			Not found		
Component 7	Not found			No found			5.04	0.66	0.99	4.97	0.99	1.00

Component 4 and Component 5 whose intensities changed non-monotonically as a function of total Cu(II) concentration appeared to have two types of binding sites, forming strong complexes with Cu(II) at very low Cu(II) concentration. This situation was similar to some previous studies (Balistrieri and Blank, 2008; Cabaniss, 2011; Di Toro et al., 2001; Meylan et al., 2004). The binding of Cu(II) by the strongly complexing functionalities (operationally denoted as Sites I) associated with Components 4 and 5 in the EEM of SRNOM and SRHA led to an enhancement of the fluorescence intensity of the components. However, upon further Cu(II) addition, complexation by other binding sites (denoted as Sites II) found in the same fluorophores causes relatively weaker complexes to form. The binding of Cu(II) by Sites II in Component 4 and 5 caused a pronounced quenching of the fluorescence associated with these components. The two components exhibited a monotonic quenching or enhancement required for complexation modeling (Figure 4a and d).

The logarithms of the conditional stability constants (log K) for Cu(II) binding to all of the EEM components were in the range of 4.9-6.1. This is consistent with prior research (Bai et al., 2008; Esteves da Silva et al., 1998; Luster et al., 1996). The values of log K of Component 2 were highest in all samples, except for SRFA, while Component 3 had relatively lower log K and f values compared with the others in each DOM samples. Component 1 and Component 7 had relative higher f values. The properties of the constituents of the EEM of SRFA and SRHPiA were relatively close, with only slight difference between the values of the equilibrium constants.

It needs to emphasize that interaction of Cu(II) with DOM was quantified based on the changes of contributions of the PARAFAC components emerged during and constituting entire EEMs obtained at varying total Cu(II) concentrations in this study, This allows examining changes of EEM more accurately and eliminating the issue of the overlap of dissimilar EEM components.

Changes of the fluorescence intensity at the combination wavelength corresponding to PARAFAC component peaks as well as the results of modeling of their behavior based on

the Ryan and Weber equation (solid line) for SRFA are shown in Figure 5. It shows that the extent of fluorescence decreased more significantly with the concentrations of Cu(II) addition compared with that in the Figure 4 (g) due to overlapping of discrete components. The equilibrium constants calculated using eq. (1) and (2) through the two approaches are compared in Table 2. These data show that the values of log K and f for each PARAFAC model component were smaller than those obtained using discrete $\lambda_{ex}/\lambda_{em}$ combinations while the correlation coefficients R^2 obtained using entire PARAFAC components' contributions were somewhat larger. This indicates that the approach utilized in this study can yield more accurate estimations of the equilibria constants describing interactions of Cu(II) with dissimilar DOM components.
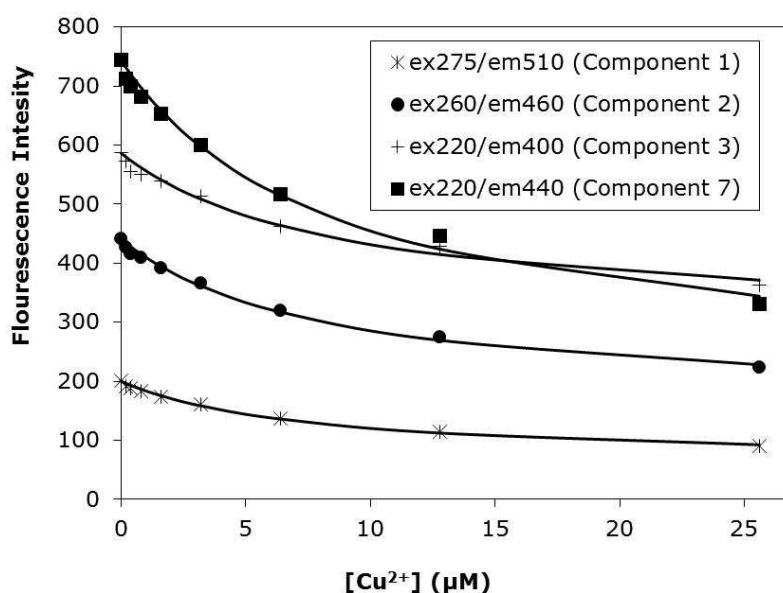

Figure 5 Fluorescence intensity at the combination wavelength corresponding to PARAFAC component peaks for SRFA (dots), and predicted by Ryan and Weber model (solid line)

Table 2 Comparison of fitting parameters of the Ryan-Weber model for SRFA, i.e., percentage of fluorescence intensity participating in the binding (f), stability constant (log K), and correlation coefficient of predicted vs. measured fluorescence intensity (R^2)

Parameter	PARAFAC model component				Corresponding intensity peak picking ($\lambda_{ex}/\lambda_{em,}$ nm/nm)			
	Component 1	Component 2	Component 3	Component 7	275/510	260/460	220/400	220/440
Log K	5.08	5.03	5.02	5.04	5.12	5.09	5.06	5.07
f	0.67	0.64	0.45	0.66	0.70	0.64	0.49	0.72
R^2	0.996	0.995	0.985	0.992	0.993	0.992	0.982	0.989

CONCLUSIONS

The following conclusions can be drawn:

The changes of EEM spectra after the addition of Cu(II) were affected by DOM. It led to the appearance of four peaks of relatively increased intensity for SRNOM and SRHA located at coordinates of $\lambda_{ex}/\lambda_{em}$ = 280 nm/350 nm, $\lambda_{ex}/\lambda_{em}$ = 250 nm/350 nm and $\lambda_{ex}/\lambda_{em}$ = 280 nm/400 nm, $\lambda_{ex}/\lambda_{em}$ = 240 nm/400 nm. On contrary, the fluorescence intensity of SRFA and SRHPiA decreased in the entire range of excitation and emission wavelengths with the addition of Cu(II), the quenching of SRFA and SRHPiA emission was more pronounced at higher emission wavelength.

The dissimilar phenomena of Cu(II) binding to DOM samples could be deconvoluted by PARAFAC. Seven independent EEM components were determined by PARAFAC to be present in the examined SRNOM, SRHA, SRFA, and SRHPiA, with varying prominence and numbers in different samples. The differences in metal binding properties for DOM samples could be discerned via the behavior of individual DOM components.

This study indicates that the method of fluorescence excitation–emission matrix (EEM) combined with PARAFAC is a promising approach to gain better insight into the interactions between trace metals and specific groups of DOM fluorophores, and can yield more accurate estimations of the equilibria constants describing interactions of Cu(II) with dissimilar DOM components.

ACKNOWLEDGEMENTS

REFERENCES

Bai, Y.C., Wu, F.C., Liu, C.Q., Li, W., Guo, J.Y. and Fu, P.Q. (2008). Ultraviolet absorbance titration for determining stability constants of humic substances with Cu(II) and Hg(II). *Analytica Chimica Acta*, 616(1), 115-121.

Baken, S., Degryse, F., Verheyen, L., Merckx, R. and Smolders, E. (2011). Metal Complexation Properties of Freshwater Dissolved Organic Matter Are Explained by Its Aromaticity and by Anthropogenic Ligands. *Environmental Science and Technology*, 45(7), 2584-2590.

Balistrieri, L.S. and Blank, R.G. (2008). Dissolved and labile concentrations of Cd, Cu, Pb, and Zn in the South Fork Coeur d'Alene River, Idaho: Comparisons among chemical equilibrium models and implications for biotic ligand models. *Applied Geochemistry*, 23(12), 3355-3371.

Browne, B.A. and Driscoll, C.T. (1993). Ph-Dependent Binding of Aluminum by a Fulvic-Acid. *Environmental Science and Technology*, 27(5), 915-922.

Cabaniss, S.E. (1992). Synchronous Fluorescence-Spectra of Metal-Fulvic Acid Complexes. *Environmental Science and Technology*, 26(6), 1133-1139.

Cabaniss, S.E. (2011). Forward Modeling of Metal Complexation by NOM: II. Prediction of Binding Site Properties. *Environmental Science and Technology*, 45(8), 3202-3209.

Chen, W., Westerhoff, P., Leenheer, J.A. and Booksh, K. (2003). Fluorescence excitation - Emission matrix regional integration to quantify spectra for dissolved organic matter. *Environmental Science and Technology*, 37(24), 5701-5710.

Christensen, J.H., Hansen, A.B., Mortensen, J. and Andersen, O. (2005). Characterization and matching of oil samples using fluorescence spectroscopy and parallel factor analysis. *Analytical Chemistry*, 77(7), 2210-2217.

Coble, P.G. (1996). Characterization of marine and terrestrial DOM in seawater using excitation

emission matrix spectroscopy. *Marine Chemistry*, 51(4), 325-346.

Cook, R.L. and Langford, C.H. (1995). Metal-Ion Quenching of Fulvic-Acid Fluorescence Intensities and Lifetimes-Nonlinearities and a Possible 3-Component Model. *Analytical Chemistry*, 67(1), 174-180.

Cory, R.M. and McKnight, D.M. (2005). Fluorescence spectroscopy reveals ubiquitous presence of oxidized and reduced quinones in dissolved organic matter. *Environmental Science and Technology*, 39(21), 8142-8149.

Di Toro, D.M., Allen, H.E., Bergman, H.L., Meyer, J.S., Paquin, P.R. and Santore, R.C. (2001). Biotic ligand model of the acute toxicity of metals. 1. Technical basis. *Environmental Toxicology and Chemistry*, 20(10), 2383-2396.

Dryer, D.J., Korshin, G.V. and Fabbricino, M. (2008). In situ examination of the protonation behavior of fulvic acids using differential absorbance spectroscopy. *Environmental Science and Technology*, 42(17), 6644-6649.

Esteves da Silva, J.C.G., Machado, A.A.S.C., Oliveira, C.J.S. and Pinto, M.S.S.D.S. (1998). Fluorescence quenching of anthropogenic fulvic acids by Cu(II), Fe(III) and UO_2^{2+}. *Talanta*, 45(6), 1155-1165.

Gamble, D.S., Underdown, A.W. and Langford, C.H. (1980). Copper(II) Titration of Fulvic-Acid Ligand Sites with Theoretical, Potentiometric, and Spectrophotometric Analysis. *Analytical Chemistry*, 52(12), 1901-1908.

Gustafsson, J.P. and Kleja, D.B. (2005). Modeling salt-dependent proton binding by organic soils with the NICA-Donnan and Stockholm Humic models. *Environmental Science and Technology*, 39(14), 5372-5377.

Hall, G.J., Clow, K.E. and Kenny, J.E. (2005). Estuarial fingerprinting through multidimensional fluorescence and multivariate analysis. *Environmental Science and Technology*, 39(19), 7560-7567.

Korshin, G., Chow, C.W.K., Fabris, R. and Drikas, M. (2009). Absorbance spectroscopy-based examination of effects of coagulation on the reactivity of fractions of natural organic matter with varying apparent molecular weights. *Water Research*, 43(6), 1541-1548.

Kumke, M.U., Tiseanu, C., Abbt-Braun, G. and Frimmel, F.H. (1998). Fluorescence decay of natural organic matter (NOM)-influence of fractionation, oxidation, and metal ion complexation. *Journal of Fluorescence*, 8(4), 309-318.

Leenheer, J.A. and Croue, J.P. (2003). Characterizing aquatic dissolved organic matter. *Environmental Science and Technology*, 37(1), 18a-26a.

Luster, J., Lloyd, T., Sposito, G. and Fry, I.V. (1996). Multi-wavelength molecular fluorescence spectrometry for quantitative characterization of copper(II) and aluminum(III) complexation by dissolved organic matter. *Environmental Science and Technology*, 30(5), 1565-1574.

Meylan, S., Odzak, N., Behra, R. and Sigg, L. (2004). Speciation of copper and zinc in natural freshwater: comparison of voltammetric measurements, diffusive gradients in thin films (DGT) and chemical equilibrium models. *Analytica Chimica Acta*, 510(1), 91-100.

Mobed, J.J., Hemmingsen, S.L., Autry, J.L. and McGown, L.B. (1996). Fluorescence characterization of IHSS humic substances: Total luminescence spectra with absorbance correction. *Environmental Science and Technology*, 30(10), 3061-3065.

Ohno, T., Amirbahman, A. and Bro, R. (2008). Parallel factor analysis of excitation-emission matrix fluorescence spectra of water soluble soil organic matter as basis for the determination of conditional metal binding parameters. *Environmental Science and Technology*, 42(1), 186-192.

Ohno, T. and Bro, R. (2006). Dissolved organic matter characterization using multiway spectral decomposition of fluorescence landscapes. *Soil*

Science Society of America Journal, 70(6), 2028-2037.

Patel-Sorrentino, N., Mounier, S. and Benaim, J.Y. (2002). Excitation-emission fluorescence matrix to study pH influence on organic matter fluorescence in the Amazon basin rivers. *Water Research*, 36(10), 2571-2581.

Plaza, C., Brunetti, G., Senesi, N. and Polo, A. (2006). Molecular and quantitative analysis of metal ion binding to humic acids from sewage sludge and sludge-amended soils by fluorescence spectroscopy. *Environmental Science and Technology*, 40(3), 917-923.

Pullin, M.J. and Cabaniss, S.E. (1995). Rank analysis of the pH-dependent synchronous fluorescence-spectra of six standard humic substances. *Environmental Science and Technology*, 29(6), 1460-1467.

Reynolds, D.M. (2003). Rapid and direct determination of tryptophan in water using synchronous fluorescence spectroscopy. *Water Research*, 37(13), 3055-3060.

Ryan, D.K. and Weber, J.H. (1982). Fluorescence quenching titration for determination of complexing capacities and stability-constants of fulvic-acid. *Analytical Chemistry*, 54(6), 986-990.

Seredyńska-Sobecka, B., Stedmon, C.A., Boe-Hansen, R., Waul, C.K. and Arvin, E. (2011). Monitoring organic loading to swimming pools by fluorescence excitation–emission matrix with parallel factor analysis (PARAFAC). *Water Research*, 45(6), 2306-2314.

Stedmon, C.A. and Bro, R. (2008). Characterizing dissolved organic matter fluorescence with parallel factor analysis: a tutorial. *Limnology and Oceanography-Methods*, 6, 572-579.

van Schaik, J.W.J., Persson, I., Kleja, D.B. and Gustafsson, J.P. (2008). EXAFS study on the reactions between iron and fulvic acid in acid aqueous solutions. *Environmental Science and Technology*, 42(7), 2367-2373.

Wu, F.C., Mills, R.B., Evans, R.D. and Dillon, P.J. (2004). Kinetics of metal-fulvic acid complexation using a stopped-flow technique and three-dimensional excitation emission fluorescence spectrophotometer. *Analytical Chemistry*, 76(1), 110-113.

Wu, J., Zhang, H., He, P.J. and Shao, L.M. (2011). Insight into the heavy metal binding potential of dissolved organic matter in MSW leachate using EEM quenching combined with PARAFAC analysis. *Water Research*, 45(4), 1711-1719.

Yamashita, Y. and Jaffe, R. (2008). Characterizing the interactions between trace metals and dissolved organic matter using excitation-emission matrix and parallel factor analysis. *Environmental Science and Technology*, 42(19), 7374-7379.